

# High-Pressure Diffusion Measurements by Mach-Zehnder Interferometry

Siv Killie, Bjørn Hafskjold, Odd Borgen, Signe Kjelstrup Ratkje, and Einar Hovde

Div. of Physical Chemistry, University of Trondheim, Norwegian Institute of Technology, N-7034 Trondheim Norway

The present work was initiated to study nitrogen diffusion in hydrocarbons at high temperature and pressure. Such data are needed for mathematical modeling of gas diffusion into the porous matrix of fractured oil reservoirs (da Silva and Belery, 1989). Few measurements of *mutual diffusion* coefficients of gas/oil systems at high pressures and temperatures have been reported. Erkey and Akgerman (1989) used the Taylor dispersion technique with binary mixtures of alkanes and *n*-octane in the temperature range from 31 to 162°C at 1.72 MPa. This appears to be the most accurate measurements for hydrocarbon mixtures at elevated pressures; the estimated accuracy was reported to be  $\pm 1\%$ . In addition to selected nitrogen/hydrocarbon mixtures, we have therefore included the methane/*n*-octane system to compare with the data of Erkey and Akgerman.

We chose to use the method of optical interferometry because it is sensitive, nonintrusive, and rapid. A good overview of optical methods for diffusion measurements is presented by Tyrrell and Harris (1984). In the interferometric methods, the differences in *phase* and *amplitude* between two interfering light beams are related to the *light intensity*. A *Mach-Zehnder interferometer* is particularly attractive because it allows a visualization of the cell. A *phase shift technique* has been implemented to determine the phase difference between the interfering beams. The *diffusion cell* is constructed for pressures up to 45 MPa and temperatures up to 200°C.

## Application of Mach-Zehnder Interferometry

The Mach-Zehnder interferometer used in this work is shown in Figure 1. Light from a He-Ne laser (A) is attenuated by a polarization filter (B) and expanded by a collimator (C). The parallel beam is split by the semitransparent mirror (D), recombined at the similar mirror (E), and observed by a video camera (not shown). The separate beam paths contain either a prism (F) or a mirror (G). The diffusion cell (H) is described in detail in the subsequent section.

The mirror (G) is mounted on a piezoelectric position transducer, which enables the use of the phase shift technique (see

below). The exact position of the mirror depends on an applied voltage in the range from 0 to 1,000 V, with a displacement of  $6 \times 10^{-9}$  m/V. The mirror and the piezoelectric position transducer will be called the *phase-shift mirror*.

The two beam splitters (D and E) and the phase-shift mirror are mounted in nonadjustable holders. The prism (F) may be tilted to adjust the interference fringe pattern. The two mirrors, the prism, the phase-shift mirror, and the diffusion cell are mounted on a metal base (0.40 m  $\times$  0.40 m). This base, together with the other optical components and the camera, is placed on a table (1.5 m  $\times$  1.0 m) made from a heavy stone slab on a steel frame, supported by solid rubber cushions.

The basic interferometric method was combined with a phase detection technique developed by Kolipoulos (1981). This technique enables us to determine the light phase shift caused by a concentration change in the gas/liquid sample.

Consider a light beam traveling in the *x* direction, perpendicular to the *y, z* plane. The measured intensity at a point (*y, z*) in the interference pattern is:

$$I(y, z) = I_0(y, z) + A(y, z) \cos [\Delta\phi(y, z) + \Delta\phi_s] \quad (1)$$

where  $I_0(y, z)$  is the background intensity,  $A(y, z)$  is the amplitude of the light,  $\Delta\phi(y, z)$  is the phase difference between the sample beam and the reference beam when the phase-shift

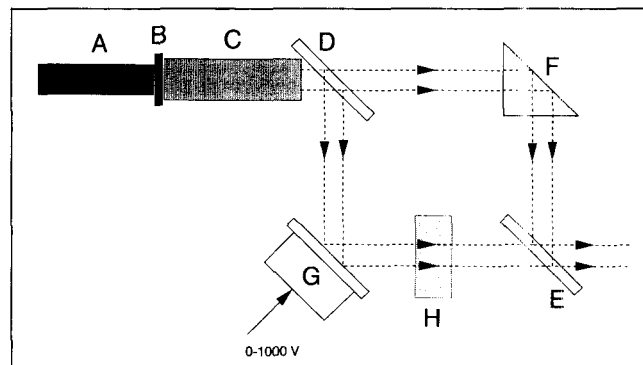


Figure 1. Setup of the Mach-Zehnder interferometer.

Correspondence concerning this article should be addressed to B. Hafskjold.  
Present address of S. Killie, Institute of Physical Chemistry and Electrochemistry II, University of Karlsruhe, Kaiserstraße 12, D-7500 Karlsruhe, Germany.

mirror is in an arbitrary zero-point position, and  $\Delta\phi_s$  is the phase shift generated by the phase-shift mirror relative to the zero-point position.

Individual contributions to  $I$  from each of the three unknown parameters,  $I_0$ ,  $A$ , and  $\Delta\phi$ , can be calculated from three or more measurements of  $I$  with known values of  $\Delta\phi_s$ . To improve the calculations, four light intensities are measured instead of three. The four intensities  $I_i$  ( $i = 1, 2, 3, 4$ ) are measured with  $\Delta\phi_s = 0, \pi/2, \pi$ , and  $3\pi/2$ , respectively. The phase shifts are performed by changing the input voltage to the phase-shift mirror between each intensity reading. Combination of the four measurements gives:

$$\Delta\phi = \arctan \left( \frac{I_4 - I_2}{I_1 - I_3} \right). \quad (2)$$

Two ambiguities exist in the calculation of the phase angle. The  $\pi$ -ambiguity occurs because Eq. 2 gives two solutions for  $\Delta\phi$  in the interval from 0 to  $2\pi$ . The phase shift technique alone provides the information needed to solve this, and the correct value of  $\Delta\phi$  can be determined as:

$$\Delta\phi_{\text{correct}} = \Delta\phi_{\text{Eq. 2}} + \pi - \text{sign}(I_4 - I_2)[1 + \text{sign}(I_1 - I_3)]\pi/2 \quad (3)$$

where  $\Delta\phi_{\text{Eq. 2}}$  is the value (in the interval from  $-\pi/2$  to  $\pi/2$ ) determined from Eq. 2.

The  $2\pi$ -ambiguity occurs because an additional solution for  $\Delta\phi$  is possible in every interval of  $2\pi$ . This can be resolved by combining the recorded intensity data with a condition on the interval between two points in time at the same location or between two locations at the same time. The condition is that the light intensity is sampled frequently enough (or at sufficiently close locations) to give a maximum change in  $\Delta\phi$  of  $2\pi$  under ideal circumstances. A maximum of  $\pi$  is recommended if the signal is noisy.

The phase shift technique requires that the conditions at each point in the image are constant during the phase stepping procedure. It is therefore necessary to perform the phase stepping, detection, and data storage in as short time as possible, which for practical reasons is limited to 600 ms for a total cycle of four steps.

## High-Pressure, High-Temperature Equipment

The high-pressure diffusion cell is shown in Figure 2. The cell body (A) and the lids (B) are constructed of aluminum bronze, which has high mechanical strength and good thermal conductivity. The cell body has channels for electric heating and thermal control (C), and temperature measurement (D). The diffusion cell is equipped with sapphire windows (E) for optical measurements and observation of the diffusion process. A Vespel frame insert (F) constitutes the walls of the diffusion compartment, which has the dimensions 8 mm  $\times$  10.5 mm  $\times$  13 mm. The thrust bushings (G) are made from stainless steel. All O-ring seals are made from Viton.

The cell was designed for 45 MPa and pressure tested up to 70 MPa. The temperature controller used in these experiments is of type Coreci, digital controller Microcor IIIA. The temperature stability was found to be about  $\pm 0.05^\circ\text{C}$ .

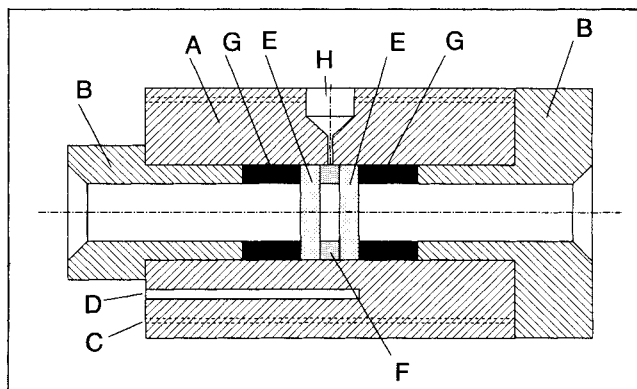


Figure 2. High-pressure, high-temperature diffusion cell.

## Instrumentation

The purpose of the instrumentation is to measure light intensities, temperature, and pressure, and to control the piezo-electric mirror during the diffusion process. The interference pattern is picked up by a Pulnix TM-34KC video camera. The video signal can be recorded by a Luxor 9272 video recorder and replayed for a closer inspection of the image during data analysis. The video signal can also be monitored, which is particularly useful during the initial stages of an experiment.

The output signal from the camera is a standard (50 frames/s, 625 lines, PAL) monochrome European video signal. It is processed by a Matrox PIP-1024 real-time image digitizer card located in an Olivetti M24 personal computer. The card digitizes the video signal by an eight-bit analog-to-digital converter. The card has a buffer capacity of four images of 512  $\times$  512 pixels. Each of the four images represents one setting of the phase-shift mirror.

The computer also contains a Burr-Brown PCI 20000 series instrumentation card used to control the phase-shift mirror with a Burleigh PZ-70 DC high-voltage operational amplifier. The instrumentation card is also used to record temperature data from a Unisystem Pt 100 temperature meter U1411 and pressure data from a Setra 204 pressure transducer. The resistance element's operating range is from  $-199.99$  to  $199.99^\circ\text{C}$  with an accuracy of  $\pm 0.02^\circ\text{C}$ . The pressure transducer operates in the range from 0 to 68 MPa.

## Experimental Studies

All chemicals were used without special purification or other treatments. Nitrogen, 99.99% (Norgas, Oslo), and methane, 99.95% (Norsk Hydro, Oslo), were supplied from pressurized gas bottles. The liquids *n*-octane, >99% (Merck, Darmstadt, art. no. 806910), and *n*-decane, >99% (Merck, Darmstadt, art. no. 803405) were loaded from open glass beakers.

A batch of dissolved gas in hydrocarbon was prepared prior to the experiment and stored at high pressure. Subsequently, the following procedure was taken:

- The gas/hydrocarbon solution was injected into the diffusion cell until the cell was completely filled.
- The cell was heated at constant pressure, and the system was allowed to stabilize for some hours.
- Parameters required for data acquisition and analysis were selected: total acquisition time, sampling frequency, the number of measuring points (see next section), top and bottom

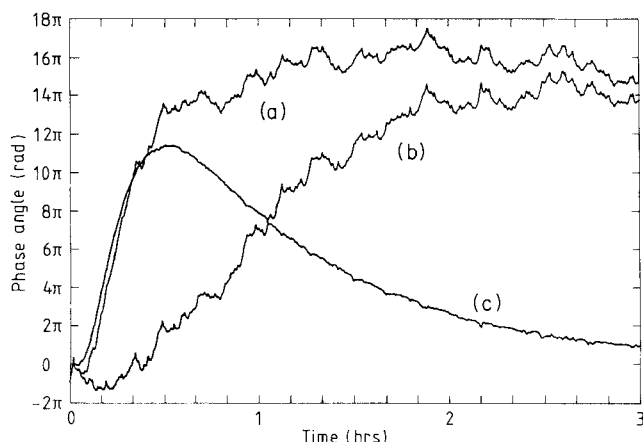


**Figure 3. Experimental changes in phase angle as function of time calculated for two points in the image (a and b) and difference between the two sets of data (c).**

coordinates of the diffusion compartment in the observed image of the cell, and coordinates of the measuring points.

- Pure hydrocarbon, preheated to the cell temperature was injected into the diffusion cell. The mixing zone between the gas solution and the pure hydrocarbon was minimized by injecting slowly. The position of the initial boundary between the two solutions was determined from the amount of pure hydrocarbon injected. The data acquisition was started simultaneously with the injection. The experiment could be run at constant pressure or constant volume, depending on whether the valve to the gas reservoir was left open or closed during the experiment.

- The system was then left on automatic control and data acquisition for as long as required for the data analysis, typically 2–3 hours for nitrogen diffusion in hydrocarbon (see Figure 3).

### Data Analysis

Data were analyzed in two steps: First, the phase angles were calculated, and then the diffusion coefficient was determined from the phase angles.

We assumed that the refractive index is a linear function of the gas concentration in the solution over the concentration range of interest. This means that the equation for concentration as a function of time (Crank, 1975) can be expressed in terms of the phase shift  $\Delta\phi$ , leading to:

$$\Delta\phi = \Delta\phi_u + \frac{1}{2}(\Delta\phi_d - \Delta\phi_u) \sum_{n=-\infty}^{\infty} \left( \operatorname{erf} \frac{l + 2nh - z}{2\sqrt{Dt}} + \operatorname{erf} \frac{l - 2nh + z}{2\sqrt{Dt}} \right) \quad (4)$$

where  $h$  is the height of the diffusion cell,  $l$  is the position (in the  $z$  direction) of the initial boundary,  $t$  is the time,  $z$  the position (in the  $z$  direction) of the measuring point, and  $\Delta\phi_u$  and  $\Delta\phi_d$  the initial values of the phase shift on each side of the initial solution boundary. Although the initial phase shifts  $\Delta\phi_u$  and  $\Delta\phi_d$  are not constants of  $y$  and  $z$ , they may be con-

sidered as *parameters* independent of time. With  $\Delta\phi$  determined experimentally as described previously these two parameters and  $D$  can be determined by a regression analysis.

The signal-to-noise ratio was improved by using the difference in the phase shifts between two measuring points in the diffusion cell. Each measuring point was taken as an average over  $5 \times 5$  pixels to further reduce noise. The equipment described earlier permits data acquisition from the entire image, but this capability was not implemented in this work.

Applying Eq. 4 to the phase shift in each measuring point, the difference becomes:

$$\Delta\phi_2 - \Delta\phi_1 = \text{constant} + \frac{1}{2}(\Delta\phi_d - \Delta\phi_u) \cdot \Sigma \quad (5)$$

where the “constant” term has been introduced to account for imperfections in the optical equipment, and

$$\Sigma = \sum_{n=-\infty}^{\infty} \left( \operatorname{erf} \frac{l + 2nh - z_2}{2\sqrt{Dt}} + \operatorname{erf} \frac{l - 2nh + z_2}{2\sqrt{Dt}} - \operatorname{erf} \frac{l + 2nh - z_1}{2\sqrt{Dt}} - \operatorname{erf} \frac{l - 2nh + z_1}{2\sqrt{Dt}} \right), \quad (6)$$

and  $\Delta\phi_1$  and  $\Delta\phi_2$  are changes in phase shift relative to the initial values at points 1 and 2, respectively. Using  $\frac{1}{2}(\Delta\phi_d - \Delta\phi_u)$  and the constant term as adjustable parameters, and the calculated value for the series term  $\Sigma$  for each value of  $t$  as the free variable, we determined the best least squares fit to the experimental data for  $(\Delta\phi_2 - \Delta\phi_1)$  for a chosen value of  $D$ . This procedure was repeated for several values of  $D$ , and the one that gave the best fit was taken as the experimental value.

### Results and Discussion

Experimental data from a nitrogen/*n*-octane experiment are shown in Figure 3 to illustrate the data analysis. Curves a and b show  $\Delta\phi$  for the individual measuring points. It is seen that a major part of the noise is canceled in the *difference curve* (c). The noise can be attributed to temperature fluctuations. A good signal-to-noise ratio is obtained for sampling points that are not too close to each other. On the other hand, both points must be sufficiently far from the initial boundary between the solutions to avoid the  $2\pi$  ambiguity, as described previously.

The diffusion coefficient was, in this particular case, determined to  $6.41 \times 10^{-9} \text{ m}^2 \cdot \text{s}^{-1}$ . This value gave the best fit of  $(\Delta\phi_2 - \Delta\phi_1)$  to the experimental data as shown in Figure 4.

A mixing zone is created when pure hydrocarbon is injected into the solution-filled cell. The consequence of this was analyzed by shifting the time scale according to the method of Longworth (1947). A selected data set from the methane/*n*-octane measurements gave an optimal time shift of 70 seconds, leading to a 6% lowering of the estimated diffusion coefficient.

Experiments were carried out for the systems nitrogen/*n*-octane, nitrogen/*n*-decane, and methane/*n*-octane. All the reported data were obtained without any time shift to correct for the initial mixing zone. Two to seven parallel experiments were made for each temperature. The results are given in Table

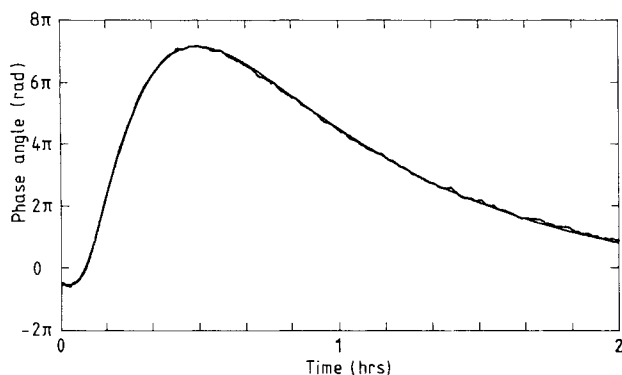


**Figure 4. Best theoretical fit to experimental data in a nitrogen/*n*-octane experiment with diffusion coefficient  $D = 6.41 \cdot 10^{-9} \text{ m}^2 \cdot \text{s}^{-1}$ .**

1, where the uncertainties listed are given as two standard deviations.

The nitrogen/*n*-octane system was studied at a constant pressure of 15 MPa for various temperatures in the range from 30 to 150°C. Pure octane was injected into mixtures of octane and nitrogen, with concentrations in the range from 4 to 7 mol %.

The nitrogen/*n*-decane experiments were carried out at constant pressures of 7.5 and 15 MPa for temperatures in the range from 25 to 150°C. Pure decane was injected into mixtures of decane and nitrogen, with concentrations in the range from 5 to 10 mol %. The difference between the two sets of data gives a pressure dependence of the diffusion coefficient of  $-0.01\%/ \text{MPa}$ . The variation is, however, not significant, since it is within the reproducibility of the values of  $D$ .

The constant-pressure experiments described so far appeared to have a flaw at  $T \geq 100^\circ\text{C}$ ; an abnormal shoulder occurred in the difference curve corresponding to that shown in Figure 3. The consequence was a poor fit. The problem became more pronounced at higher temperatures. An experiment carried out with nitrogen/*n*-decane at 75°C and constant volume with initial pressure of 15 MPa gave a 4% lower diffusion coefficient as compared to the constant-pressure result, and the curve fitting seemed to be somewhat better. During this experiment, the pressure decreased in the diffusion cell. This indicates that a volume contraction had occurred during the constant pressure experiments. We consider the experimental conditions given by constant volume as better defined from a practical as well as theoretical point of view, since the constant volume is a defined reference frame in a diffusion experiment. No correction for the moving boundary was made in any of the experiments.

The methane/*n*-octane experiments were carried out at constant volume, with a concentration range from 0 to 5 mol %, at 1.72 MPa initial pressure and for temperatures in the range from 25 to 150°C. The results by Erkey and Akgerman (1989) are within a 95% confidence interval of our results for temperatures below some 120°C. The sum of systematic errors analyzed here leads to a 10% overestimate of  $D$  in the constant-pressure results and a 6% overestimate in the constant-volume results. The random errors add another  $\pm 10\%$  to the uncertainties. Considering our estimated uncertainties, the agreement with Erkey and Akgerman, who report 1% uncertainty in their results, is somewhat unexpected.

**Table 1. Measured Diffusion Coefficients\***

Temp. K	Diff. Coeff. $10^{-9} \text{ m}^2 \cdot \text{s}^{-1}$	
<i>Nitrogen in n-Octane at 15 MPa (<math>E_a = 4.2 \pm 0.8 \text{ kJ} \cdot \text{mol}^{-1}</math>)</i>		
303.1	5.5	(1)
324.8	$7.7 \pm 0.9$	(7)
373.2	$12.3 \pm 0.1$	(2)
$399.3 \pm 0.3$	$15.3 \pm 0.3$	(2)
$423 \pm 1$	$17 \pm 1$	(2)
<i>Nitrogen in n-Decane at 7.5 MPa (<math>E_a = 5.0 \pm 0.3 \text{ kJ} \cdot \text{mol}^{-1}</math>)</i>		
297.5	$4.75 \pm 0.08$	(4)
322.3	$6.6 \pm 0.2$	(4)
346.9	$8.6 \pm 0.1$	(4)
371.8	$12 \pm 1$	(4)
396.5	$15 \pm 1$	(4)
$421.5 \pm 0.5$	$19 \pm 1$	(3)
<i>Nitrogen in n-Decane at 15 MPa (<math>E_a = 5.0 \pm 0.8 \text{ kJ} \cdot \text{mol}^{-1}</math>)</i>		
297.4	$4.5 \pm 0.2$	(4)
321.9	$5.9 \pm 0.2$	(5)
$347.5 \pm 0.5$	$7.8 \pm 0.3$	(4)
371.7	$10.4 \pm 0.4$	(6)
396.4	$14 \pm 1$	(4)
420.9	$19 \pm 4$	(4)
<i>Methane in n-Octane at 1.72 MPa (<math>E_a = 5.2 \pm 0.7 \text{ kJ} \cdot \text{mol}^{-1}</math>)</i>		
301.4	$6.3 \pm 0.3$	(3)
322.1	$8.4 \pm 0.4$	(4)
$347.2 \pm 0.2$	$10.9 \pm 0.1$	(4)
373.2	$14 \pm 1$	(3)
$397.8 \pm 0.3$	$20 \pm 2$	(4)
424.3	$25 \pm 3$	(4)

\*The number of parallel experiments is given in parentheses, and uncertainties are given as two standard deviations. The temperature is given within  $\pm 0.1 \text{ K}$ , unless otherwise specified. The activation energy determined from an Arrhenius plot is given as  $E_a$  for each system.

During these experiments, we found that the optical equipment and the phase shift technique performed reliably. The method is particularly sensitive; with the current cell, one fringe was found to correspond to a difference in mole fractions of about  $10^{-3}$ . No calibration of the equipment is necessary, but calibration against published data for KCl (aq.) will be made in our future work to assess the systematic errors. The system is closed during the experiment and it is not necessary to take samples for compositional analysis. The experiment is as fast as the process itself; one gas/liquid measurement typically takes 2–3 hours with the current cell. The fact that the sample is visible allows a continuous monitoring. An unsuccessful experiment can thus immediately be discontinued. By analyzing the data as discussed earlier, it is not necessary to know the refractive index of the system.

## Acknowledgment

Financial support from The Norwegian Research Council for Science and Humanities, The Norwegian Institute of Technology, and FINA Exploration Norway A/S is appreciated.

## Notation

$A(y, z)$  = amplitude of light at point  $(y, z)$   
 $D$  = diffusion coefficient,  $\text{m}^2 \cdot \text{s}^{-1}$   
 $h$  = height of diffusion cell, m

$I(y, z)$  = intensity at point  $(y, z)$   
 $I_0(y, z)$  = background intensity at point  $(y, z)$   
 $l$  = position of the initial solution boundary in diffusion cell, m  
 $t$  = time, s

### Greek letters

$\Delta\phi(y, z)$  = phase difference between sample beam and reference beam when the piezoelectric mirror is in the zero point position  
 $\Delta\phi_d$  = initial phase shift in lower part of the cell  
 $\Delta\phi_s$  = phase shift generated by the phase-shift mirror  
 $\Delta\phi_u$  = initial phase shift in upper part of the cell  
 $\omega$  = frequency of monochromatic light,  $s^{-1}$

Erkey, E., and A. Akgerman, "Translational-Rotational Coupling Parameters for Mutual Diffusion in *n*-Octane," *AIChE J.*, **35**, 443 (1989).

Kolipoulos, C. L., "Interferometric Optical Phase Measurement Techniques," PhD Thesis, Univ. of Arizona, Tucson (1981).

Longworth, L. G., "Experimental Test of an Interference Method for the Study of Diffusion," *J. Amer. Chem. Soc.*, **69**, 2510 (1947).

da Silva, F. V., and P. Belery, "Molecular Diffusion in Naturally Fractured Reservoirs: A Decisive Recovery Mechanism," Paper No. 19672, Soc. of Pet. Engrs., 429 (1989).

Tyrrell, H. J. V., and K. R. Harris, *Diffusion in Liquid: A Theoretical and Experimental Study*, Butterworths, Great Britain (1984).

### Literature Cited

Crank, J., *The Mathematics of Diffusion*, 2nd ed., Oxford University Press (1975).

Manuscript received July 6, 1990, and revision received Nov. 8, 1990.